

Jason-3 GDR
Cyclic Cal/Val report

Cycle 710

2026-10-02 18:56:22 to 2026-10-12 15:40:37

Processing Baseline G v1.01

Reference: SALP-RP-MAO-OP-17755-CN-710

Nomenclature: Jason-3 GDR Cyclic Cal/Val report

Issue: 01/ 00

Date: November 12, 2026

Project:	SALP MISSION PERFORMANCE SERVICE FOR Jason-3 MISSION		
Title:	Jason-3 GDR Cyclic Cal/Val report		
Author(s):	B. Flamant, CLS J. Coquelin, ALTEN G. Thoumyre, CELAD		
Approved by:	C. Boulanger, CNES	**Application authorized by:**	N. Picot, CNES

Table of Contents

1 Introduction **4**

2 Cycle overview **5**

3 Data coverage and edited measurement **7**
3.1. Data coverage 7
3.2. Edited measurements 9

4 Geophysical parameter analysis **11**
4.1. Significant Wave Height 11
4.2. Backscattering coefficient 14
4.3. Altimeter Wind Speed 16
4.4. Ionospheric correction 18
4.5. Mispointing 20
4.6. Radiometer parameters 21

5 Crossover Analysis **23**
5.1. Mono mission crossover 23

6 Sea Surface Height Anomaly **25**

7 Mean Sea Level estimations (MSL) **26**
7.1. Global MSL trend 26
7.2. Regional MSL trends 27

8 Conclusion **28**

1 Introduction

Jason-3 satellite was successfully launched on the 17th of January 2016. In the first mission years, Jason-3 was on its operational orbit to continue the long term climate data record on the primary TOPEX, Jason-1, and OSTM/Jason-2 ground track. Until October 2nd 2016, Jason-3 and Jason-2 were in tandem flight, with only 80 seconds delay, before Jason-2 was removed from the operational orbit that was used by TOPEX from 2002 to 2005 and Jason-1 from 2009 to 2012. After tandem phase with Jason-2, Jason-3 became the reference mission in the DUACS system from mid-September 2016 onwards.

After the launch of Sentinel-6A / Michael Freilich, Jason-3 was used as a reference to perform the tandem phase between both missions. During the year 2022, the success of this tandem phase led to move Jason-3 to an interleaved orbit to leave the place to Sentinel-6A. The maneuver took place between April 7th 2022 and April 25th 2022 and it was decided to start over the cycle count at 300.

Jason-3 was put back to its reference orbit from January 30th 2025 to June 2nd 2025. During this period, Jason-3 was another time in tandem phase with Sentinel-6A to ensure the instrumental stability of both missions before the launch of Sentinel-6B.

Since June 18th 2025, Jason-3 has been in a Long Repeat Orbit (LRO).
Since then and in spite of the ageing of the instruments on-board, Jason-3 still shows an excellent performance in terms of CalVal metrics and remains a pilar of the altimetric constellation. No major anomaly was detected over 2025.

From January 30th 2025, Jason-3 operational production has transitioned from standards GDR-F to standards GDR-G1.

Previous cyclic reports and annual reports can be found in the dedicated website: https://www.aviso.altimetry.fr/en/data/calval/systematic-calval.html.

The purpose of this document is to report the major features of the data quality from the Jason-3 mission over ocean. The objectives are to:

- Provide a data quality assessment
- Provide users with necessary information for data processing
- Report any change likely to impact data quality at any level, from instrument status to software configuration
- Present the major useful results for this cycle.

2 Cycle overview

This document reports results from Jason-3 GDRs over **cycle 710, spanning from 2026-10-02 18:56:22 to 2026-10-12 15:40:37.**

This cycle has been produced with the Processing Baseline G v1.01, and the processing software references L1 library=V6.2, L2 library=V7.3p2, Processing Pilot=7.2.0.

254 netCDF pass files are provided over the 254 expected (no missing files).
POSEIDON-3B instrument onboard Jason-3 implements three main tracking modes:

- The autonomous acquisition and tracking mode,
- The DIODE acquisition and autonomous tracking mode,
- The DIODE & DEM mode.

Over cycle 710, the Jason-3 altimeter (POS-3B) operates in autonomous acquisition and tracking mode.

Over this cycle, the following events occured :

- AMR-H reset from 2026-10-05 16:38:18 to 2026-10-05 16:38:24 (pass 75, timing over land)

The main metric that describes the data quality is derived from the analysis of sea surface variability at crossovers. Using a selection to remove shallow waters (1000m), areas of high ocean variability and high latitudes (> |50°|), the crossover standard deviation over the cycle is 5.85 cm for Jason-3 MLE4. This first metric is in line with usual values that are obtained on altimetry mission.

Summary of the main performances are listed in the table 1:

Cycle 710	**MLE4**	**Adaptive**
Percentage of missing measurements over open ocean	**0.02%**	
Percentage of rejected measurements over open ocean	**15.48%**	**14.29%**
of which rejected due to sea ice	**11.91%**	
of which rejected with threshold verification (after land and ice removed)	**3.52%**	**2.30%**
Crossover standard deviation on geographical selection	**5.85cm**	**6.05cm**

Table 1: Summary of cycle 710 performances over open ocean.

3 Data coverage and edited measurement

This section presents results that illustrate data quality over this cycle. These products verifications are produced operationally, to allow long-term monitoring of missing and edited measurements.

3.1. Data coverage

The map below (Figure 1) illustrates 1Hz missing measurements relative to the satellite nominal ground track.

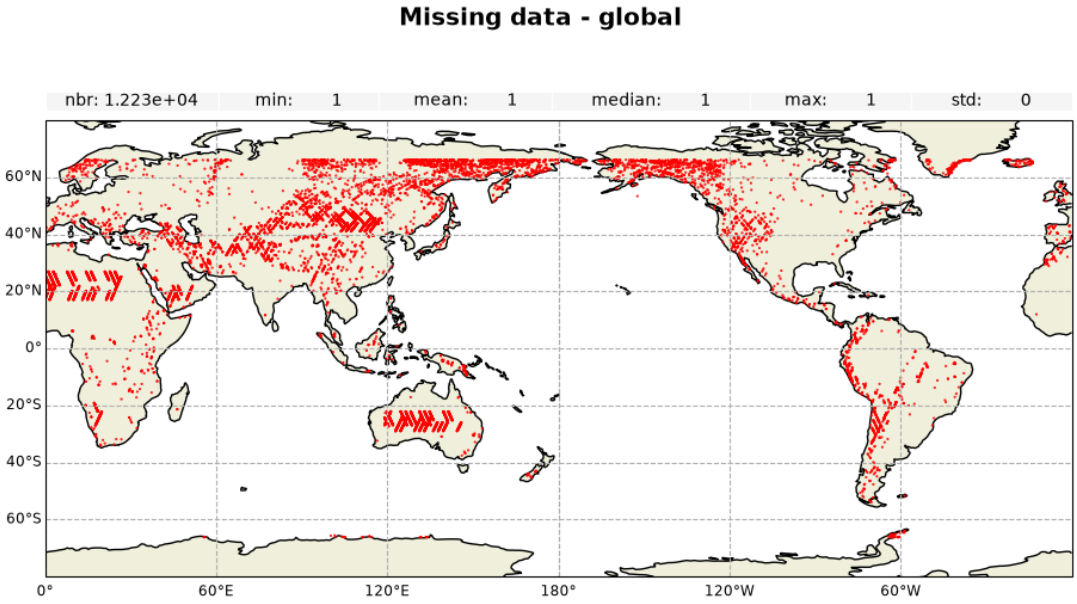


Figure 1: Map of missing measurements for Jason-3 GDR cycle 710

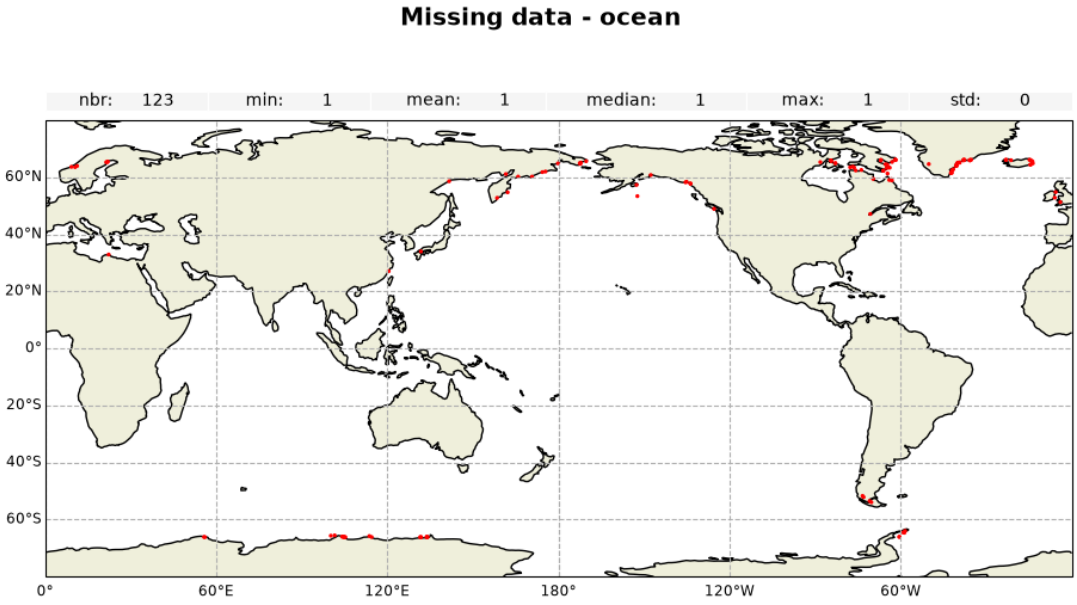


Figure 2: Map of missing measurements over ocean for Jason-3 GDR cycle 710

Over this cycle, there is missing data over ocean for :

- 123 missing points (less than 4 per pass), particularly in Northern Hemisphere.

The monitoring of the percentage of missing measurements is represented in Figure 3. Values have been computed over ocean for each track of the cycle. The mean percentage is equal to **0.02 %** over the complete cycle.

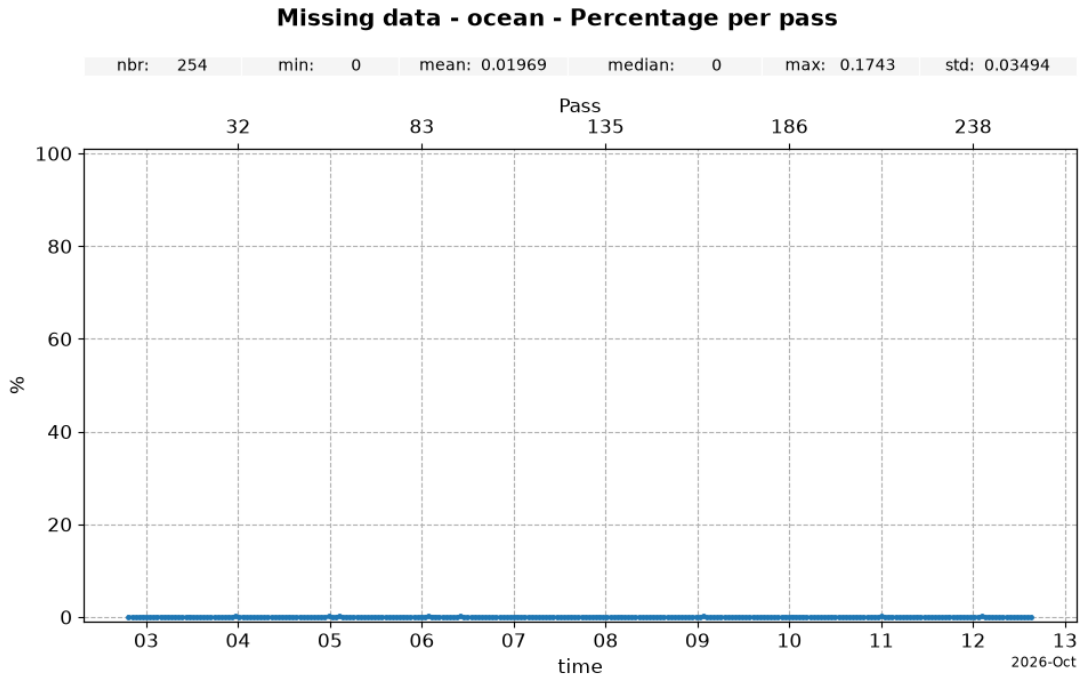


Figure 3: Monitoring of the percentage per pass of missing data over ocean for Jason-3 GDR cycle 710

3.2. Edited measurements

The editing criteria are defined as minimum and maximum thresholds for various parameters. Measurements are edited if at least one parameter exceeds the thresholds. These thresholds are expected to remain constant throughout Jason-3 mission, so that monitoring the number of edited measurements allows a survey of data quality.

The percentage of points removed by each criterion is given in the table 2. These percentages also include points with undefined values. Note that these statistics are obtained with measurements over ocean only (using surface_classification_flag) and already edited by ice flag (using ice_flag).

The percentage of measurements with sea ice is equal to **11.91 %**.

Parameters	Thresholds		Unit	Rejected (%)	
	Minimun	Maximum		MLE4	Adaptive
Sea surface height anomaly	-2	2	m	1.82	1.32
Sea surface height	-130	100	m	0.93	0.21
Range Number	10	20		1.22	0.46
Range STD	0	0.2	m	1.61	0.82
Sigma0	7	30	dB	0.71	0.35
Sigma0 Number	10	20		1.22	0.44
Sigma0 STD	0	1	dB	2.06	0.78
Significant Wave Height	0	11	m	0.77	0.77
Altimeter wind speed	0	30	$m.s^{-1}$	1.18	1.18
Sea State Bias	-0.5	0	m	0.65	0.65
Filtered ionospheric correction	-0.4	0.04	m	1.06	1.00
Square off nadir angle	-0.2	0.64	deg^2	0.71	
Equilibrium tide	-0.5	0.5	m	0.00	
Inverted barometer correction	-2	2	m	0.00	
Dry tropospheric correction	-2.5	-1.9	m	0.00	
Internal tide	-5	5	m	0.00	
Ocean tide height	-5	5	m	0.00	
Pole tide height	-15	15	m	0.00	
Solid Earth tide height	-1	1	m	0.00	
Radiometer Wet tropo correction	-0.5	-0.001	m	0.13	
Global statistics of edited measurements by thresholds				3.52 %	2.30 %

Table 2: Table of parameters used for editing and the corresponding ratio of edited measurements for Jason-3 MLE4 and Adaptive, over cycle 710

The measurements rejected during the editing process are shown on the maps below for MLE4 data (Figure 4). Equatorial wet zones or zones with sea ice appear on the maps as regions with less valid data, as it is also the case for other altimeters: measurements are corrupted by rain or sea ice. They were therefore removed by editing.

Over this cycle, no segment is rejected unexpectedly.
Nevertheles, an AMR reset induced a data gap in the WTC (passes 75 to 77) and also impacted the filtered ionospheric correction in IGDR (passes 76), this was solved in GDR.

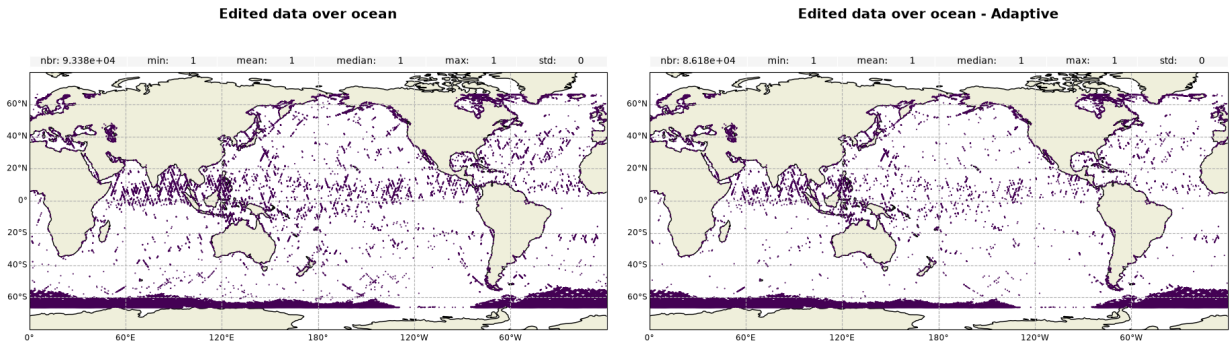


Figure 4: Edited measurements for Jason-3 over cycle 710 for MLE4 (left) and Adaptive (right)

4 Geophysical parameter analysis

The monitoring of instrumental and geophysical parameters is crucial to detect potential drifts or jumps in long-term time series. These verifications are produced operationally to allow systematic monitoring of the main relevant parameters. When possible, comparisons with ERA5 model data and/or with Sentinel-6A data are performed.

4.1. Significant Wave Height

Ku-band wave estimations derived from altimeter measurements are monitored in this section. Wave height may reach several meters. Normalized histograms over cycle are plotted on the figure below for MLE4 and Adaptive. MLE4 SWH is centered around 2.84 m for MLE4 and 2.78 m for Adaptive. It shows the consistency between the two retrackings. Furthermore, values are coherent with Sentinel-6A estimations.

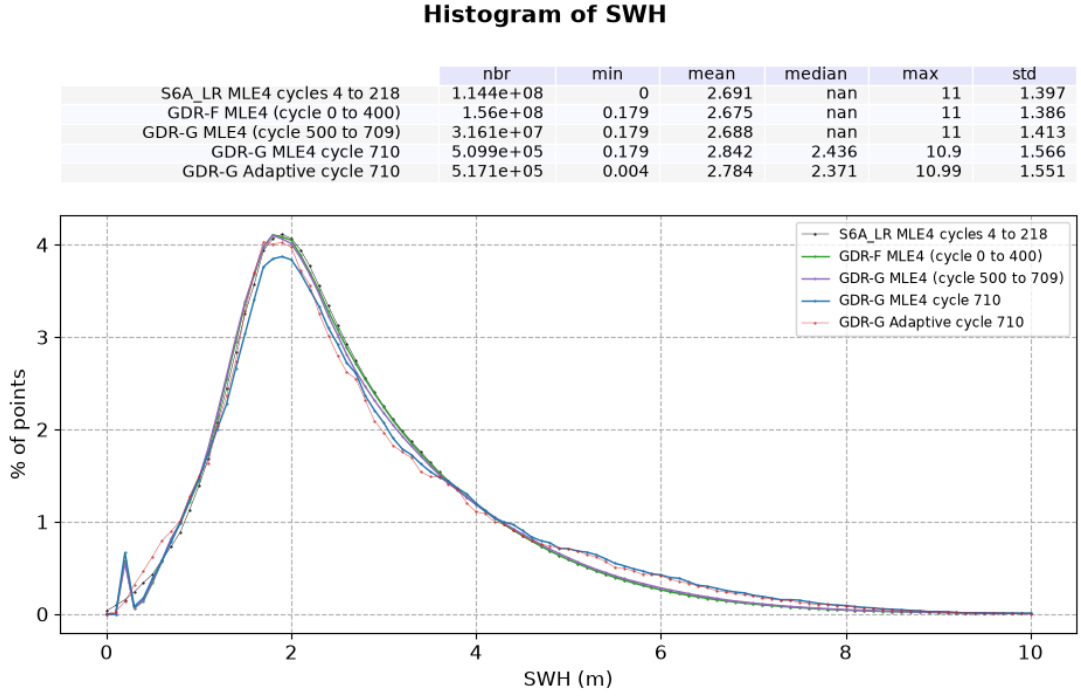


Figure 5: Comparison of Sentinel-6A, Jason-3 GDRF and GDRG records and current cyclic histogram for Significant Wave Height.

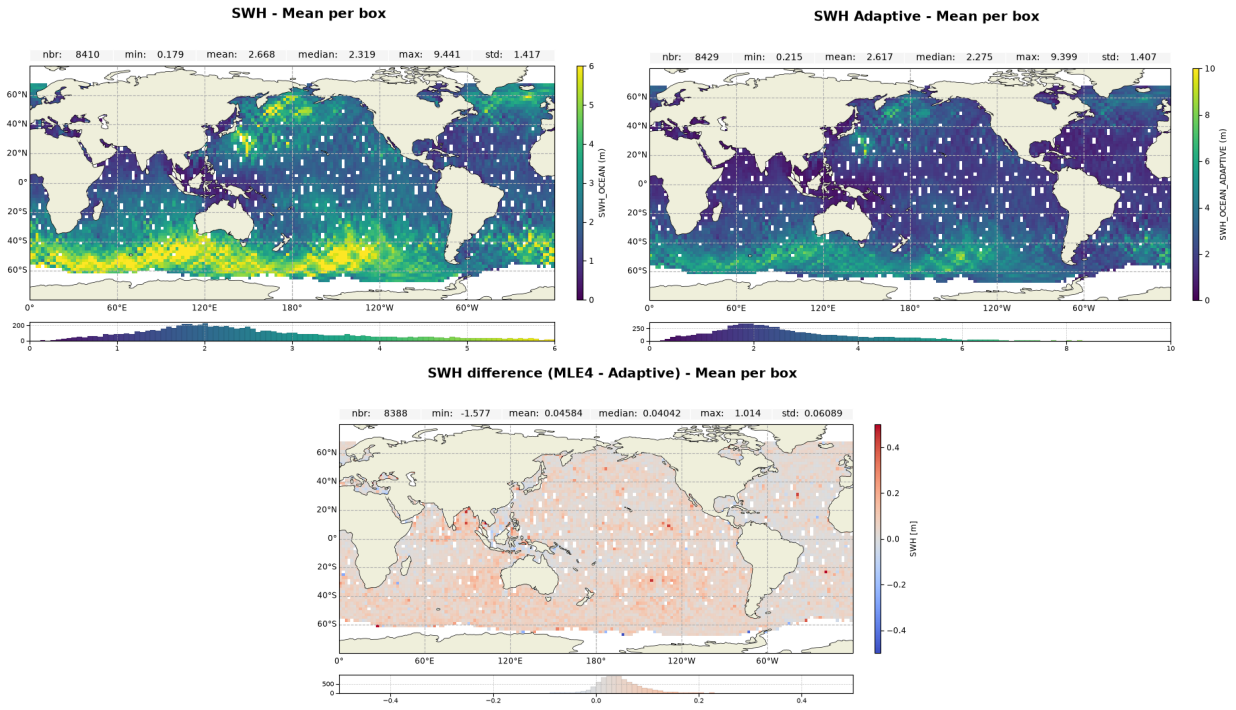


Figure 6: Map of Ku-band Significant Wave Height over cycle 710 for Jason-3 MLE4 (up left), Adaptive (up right) and difference MLE4-Adaptive (down)

The daily average of Ku-band SWH for Jason-3 is plotted on Figure 7 from cycle 001. It shows similar features between Jason-3, Sentinel-6A and ERA5 model.

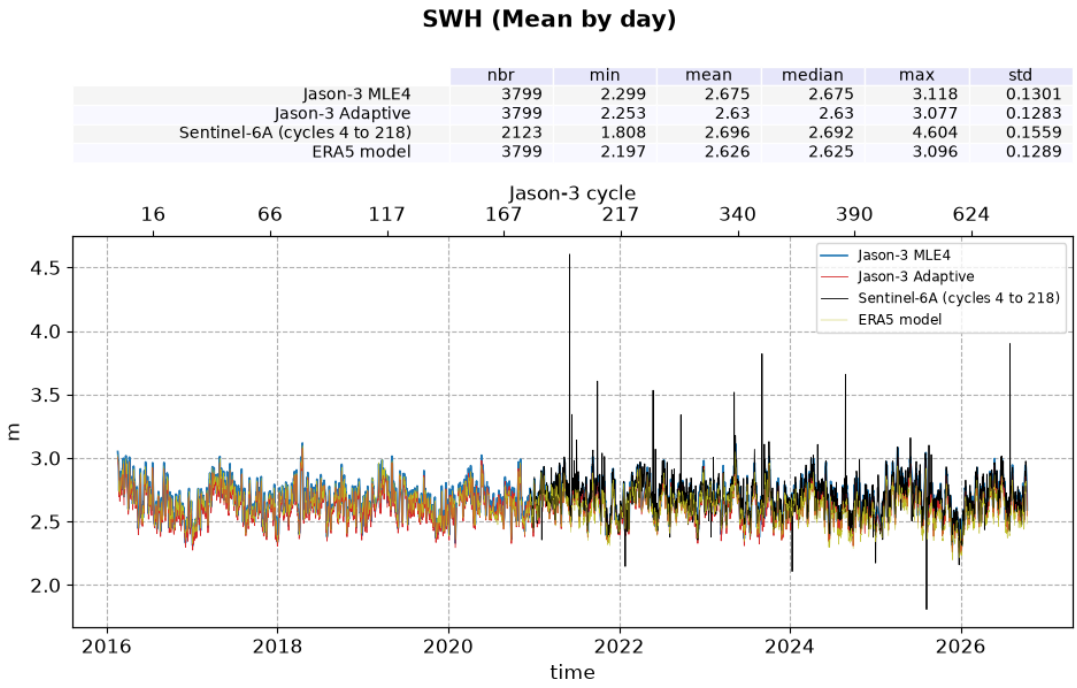


Figure 7: Ku-band Significant Wave Height daily monitoring from cycle 001 to 710, for Jason-3 and Sentinel-6A

4.2. Backscattering coefficient

Ku-band backscattering coefficient is centered around 13.67 dB for MLE4 and around 13.69 dB for Adaptive (Figure 8).

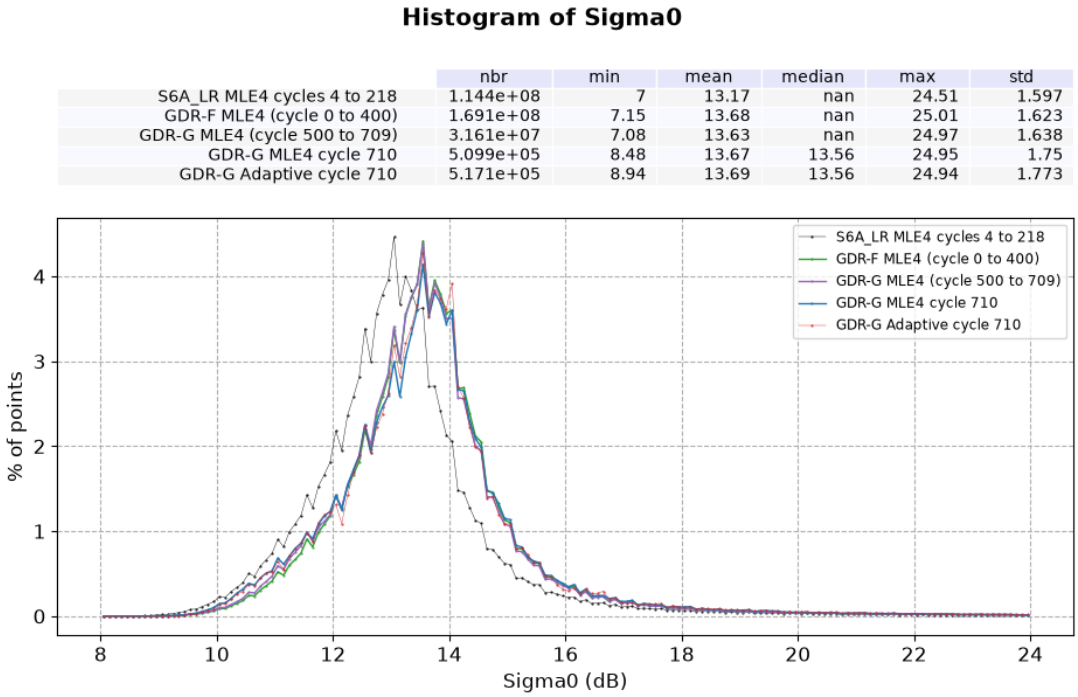


Figure 8: Ku-band Backscattering coefficient histogram computed over cycle 710

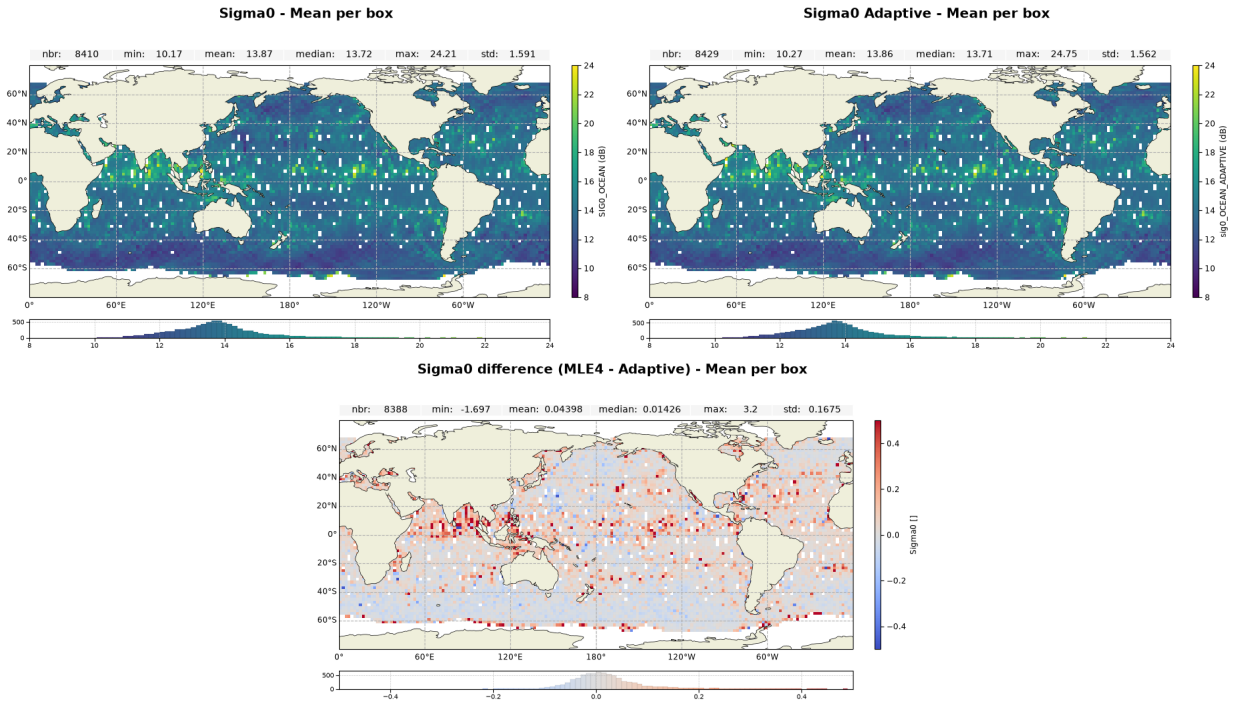


Figure 9: Map of Ku-band backscatter coefficient over cycle 710 for Jason-3 MLE4 (up left), Adaptive (up right) and difference MLE4-Adaptive (down)

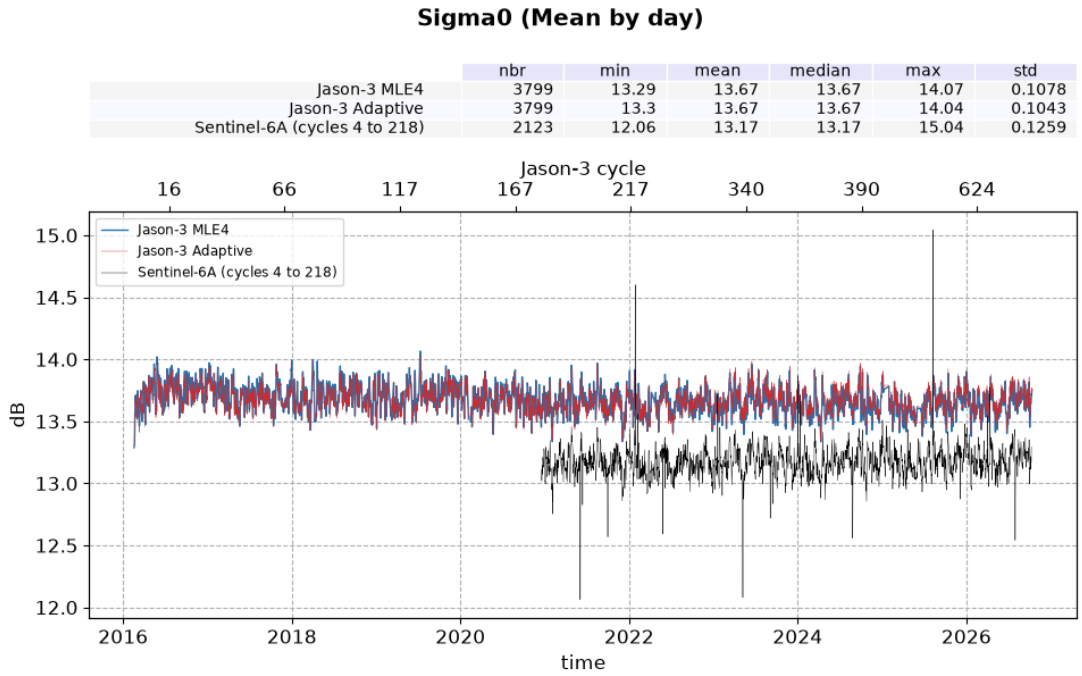


Figure 10: Ku-band Backscattering coefficient daily monitoring from cycle 001 to 710, for Jason-3 and Sentinel-6A

4.3. Altimeter Wind Speed

Altimeter wind speed is derived from backscattering coefficient and significant wave height using Collard algorithm. To allow wind speed computation, a calibration bias is applied on the backscattering coefficient. Since the switch to standard GDRG, an additional bias is applied on the backscattering coefficient to compensate the AGC drift.

Histogram of wind speed

	nbr	min	mean	median	max	std
S6A_LR MLE4 cycles 4 to 218	1.144e+08	0	8.001	nan	27.62	3.692
GDR-F MLE4 (cycle 0 to 400)	1.691e+08	0	8.041	nan	27.76	3.743
GDR-G MLE4 (cycle 500 to 709)	3.161e+07	0	8.002	nan	27.75	3.765
GDR-G MLE4 cycle 710	5.099e+05	0	7.95	7.34	25.43	3.955
GDR-G Adaptive cycle 710	5.171e+05	0	7.855	7.28	24.31	3.888

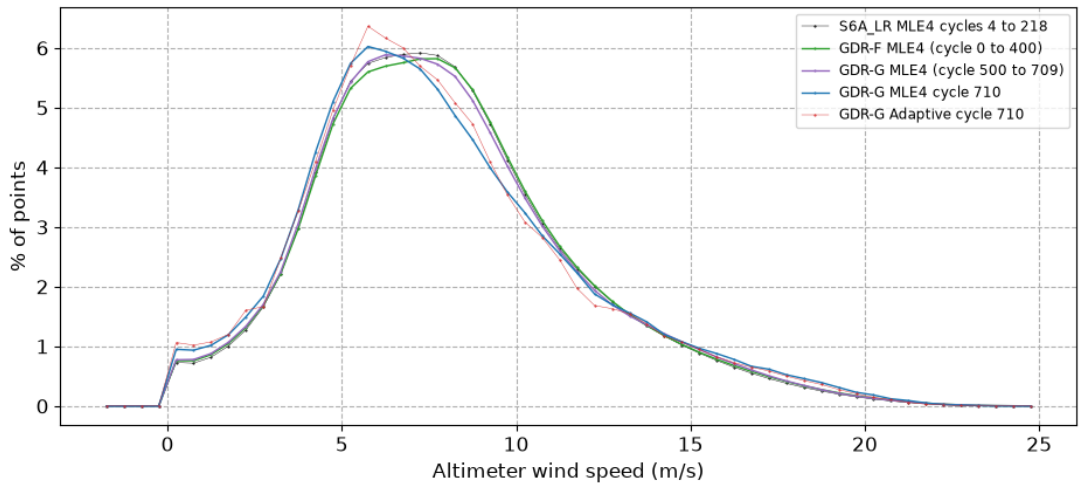


Figure 11: Altimeter Wind Speed histogram computed over cycle 710

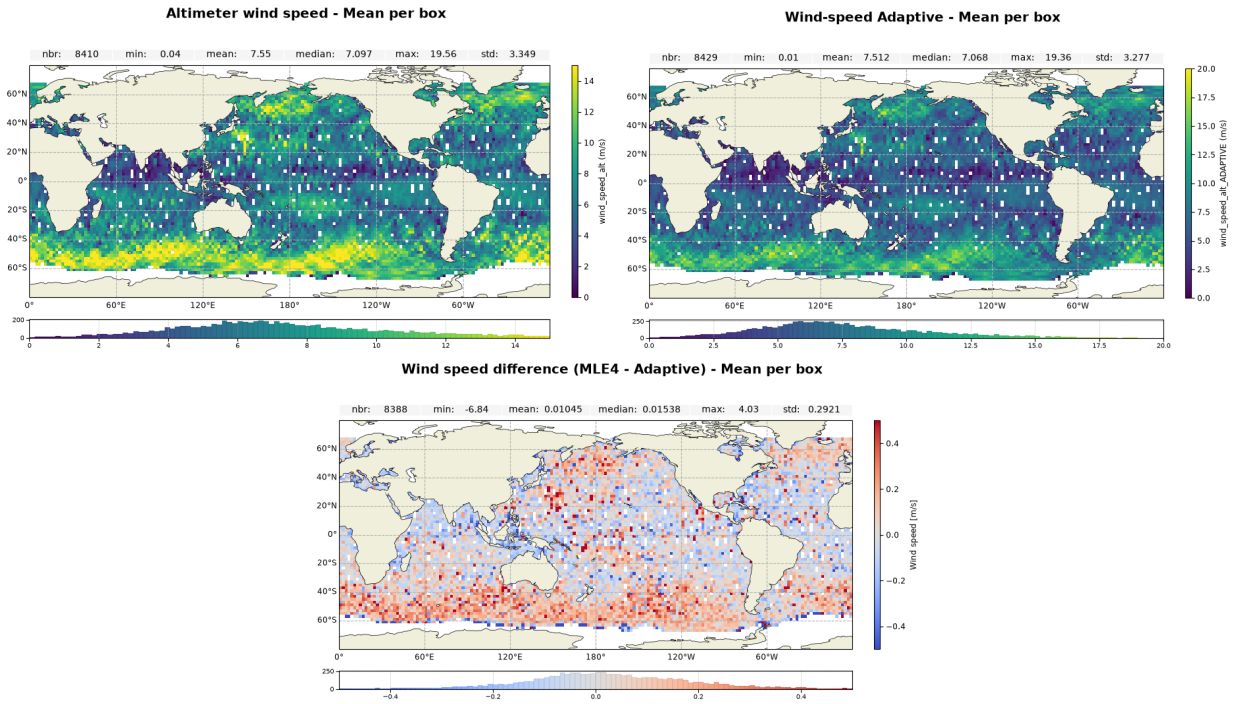


Figure 12: Map of Ku-band wind-speed over cycle 710 for Jason-3 MLE4 (up left), Adaptive (up right) and difference MLE4-Adaptive (down)

The daily average from cycle 001 shows the wind speed values centered around 8.03 m/s for MLE4 and 7.97 m/s for Adaptive. It shows similar features between Jason-3, Sentinel-6A and ERA5 model.

Altimeter wind speed (Mean by day)

	nbr	min	mean	median	max	std
Jason-3 MLE4	3799	7.074	8.034	8.038	9.027	0.2776
Jason-3 Adaptive	3799	7.063	7.971	7.979	8.914	0.2682
Sentinel-6A (cycles 4 to 218)	2123	3.438	7.998	8.003	11.43	0.3232
ERA5 model	3799	7.064	7.929	7.931	8.832	0.2612

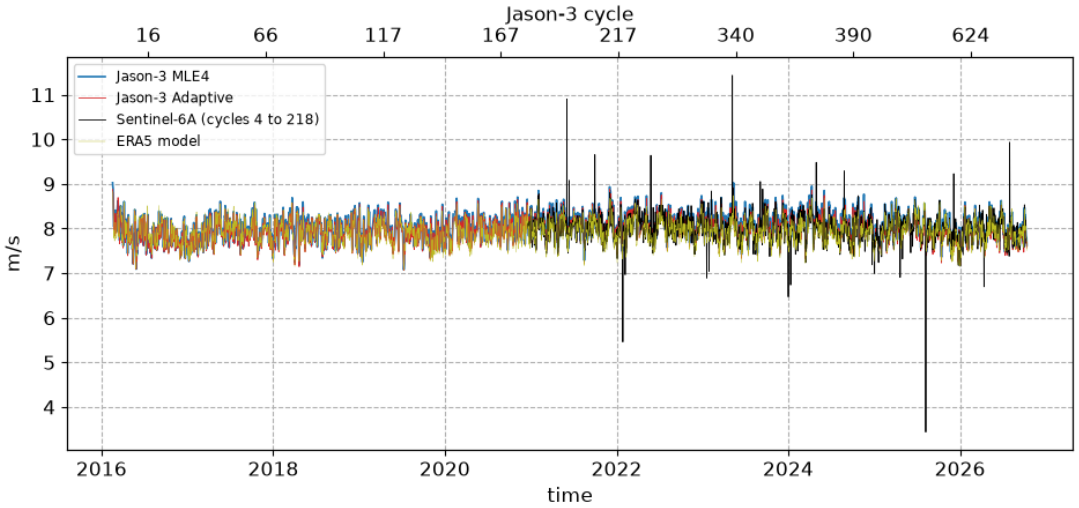


Figure 13: Wind Speed daily monitoring from cycle 001 to 710 for Jason-3 GDR, and Sentinel-6A (LR MLE4)

4.4. Ionospheric correction

Over this cycle, altimeter filtered ionospheric correction is centered around -0.04 cm for MLE4 and around -0.03 cm for Adaptive.
Jason-3 comparison with GIM model is monitored on Figure 15.

Histogram of ionospheric correction

	nbr	min	mean	median	max	std
S6A_LR MLE4 filtered solution cycles 4 to 218	1.144e+08	-0.3999	-0.04652	nan	0.04	0.0423
GDR-F filtered solution MLE4 (cycle 0 to 400)	1.691e+08	-0.3927	-0.02794	nan	0.0394	0.03396
GDR-G filtered solution MLE4 (cycle 500 to 709)	3.161e+07	-0.398	-0.04646	nan	0.0396	0.04168
GDR-G filtered solution MLE4 cycle 710	5.099e+05	-0.2013	-0.03629	-0.0214	0.0079	0.03601
GDR-G filtered solution Adaptive cycle 710	3.198e+07	-3.242	-0.04433	nan	0.8733	0.0482
GDR-F MLE4 (cycle 0 to 400)	1.691e+08	-3.271	-0.02836	nan	2.793	0.03679
GDR-G MLE4 (cycle 500 to 709)	3.161e+07	-3.268	-0.0458	nan	1.044	0.0445
GDR-G MLE4 cycle 710	5.099e+05	-1.63	-0.03557	-0.0229	0.1338	0.03959
GDR-G Adaptive cycle 710	5.171e+05	-0.2353	-0.03434	-0.0196	0.0183	0.03639
GIM model cycle 710	5.099e+05	-0.1993	-0.04882	-0.0316	-0.0049	0.03907

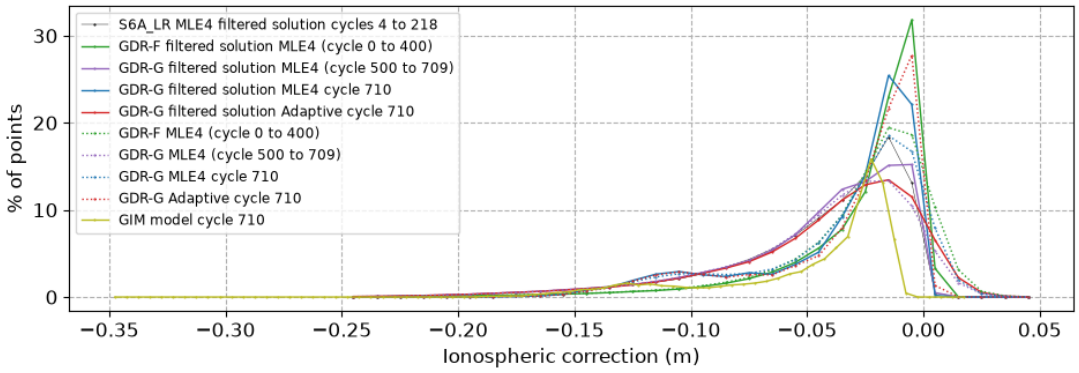


Figure 14: Histogram of altimeter ionospheric correction.

Ionospheric Correction MLE4 (Mean by day)

	nbr	min	mean	median	max	std
Jason-3 MLE4 filtered	3799	-0.1053	-0.03076	-0.02211	-0.007818	0.02039
Jason-3 MLE4 raw	3799	-0.1058	-0.03101	-0.02249	-0.008196	0.02026
Jason-3 Adaptive filtered	3799	-0.103	-0.02832	-0.01959	-0.005172	0.02052
Sentinel-6A (cycles 4 to 218)	2123	-0.1157	-0.04625	-0.04518	-0.003057	0.01956
GIM model	3799	-0.125	-0.04335	-0.03425	-0.01673	0.02272

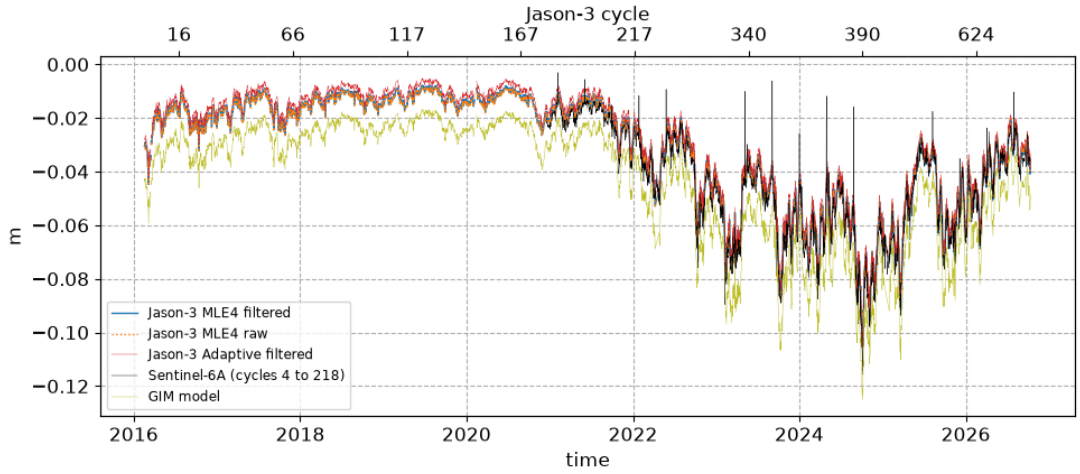


Figure 15: Daily mean of ionosphere correction over cycle 710 for Jason-3 MLE4 and Adaptive, and for Sentinel-6A

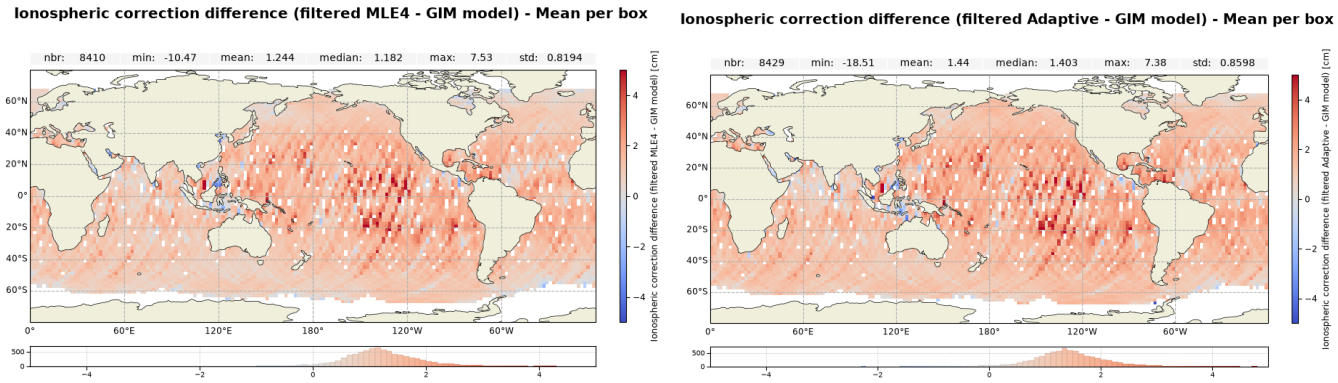


Figure 16: Ionospheric correction difference over cycle 710 for Jason-3 GDR : Filtered MLE4 - GIM model (left) and Filtered Adaptive - GIM model (right)

4.5. Mispointing

Note that as there is no square off nadir angle values on Adaptive retraking algorithm, only MLE4 values are shown here. Over this cycle, Jason-3 mispointing deduced from waveforms through MLE4 retracking is centered around 0.00 deg^2.

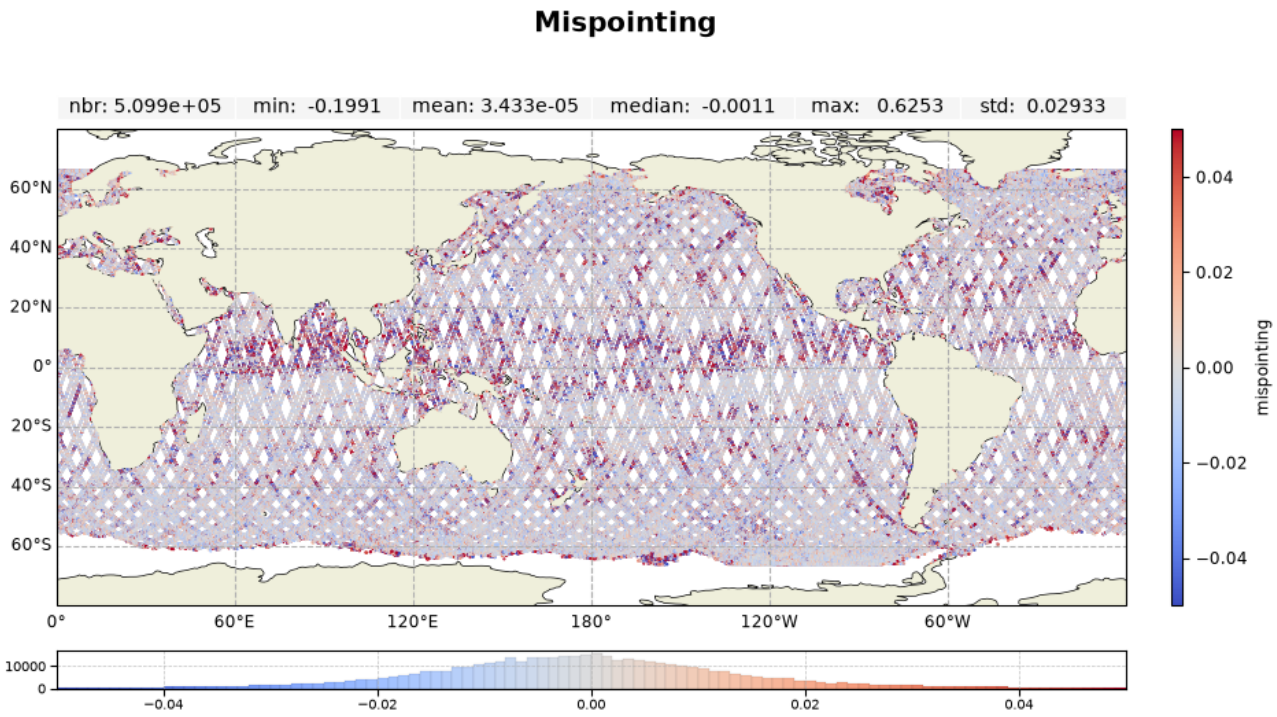


Figure 17: Along-track map of mispointing over cycle 710 for Jason-3 MLE4

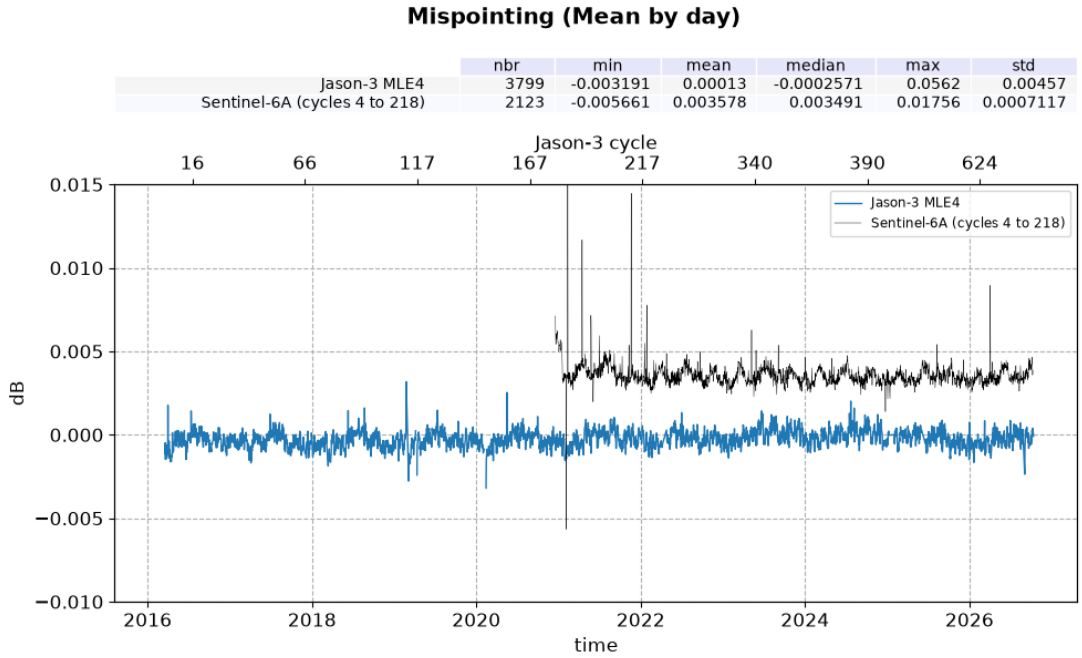


Figure 18: Mispointing daily monitoring from cycle 001 to 710 for Jason-3 GDR and Sentinel-6A

4.6. Radiometer parameters

The Wet Tropospheric Correction is derived from measurements from the radiometer. This correction is compared to the ECMWF model to assess its quality.

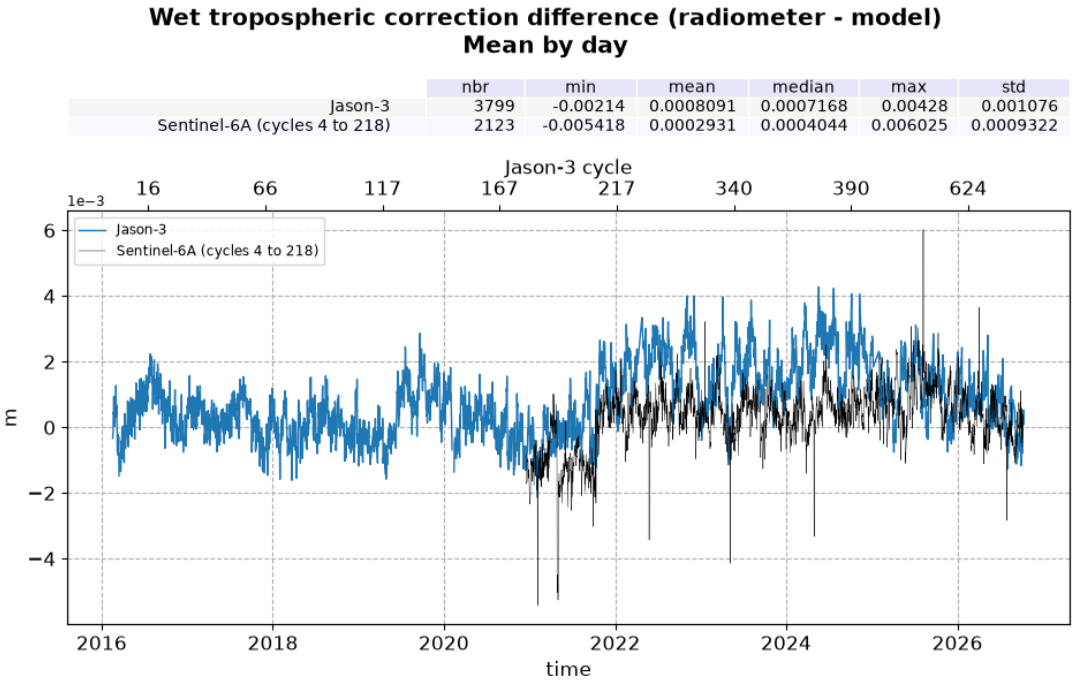


Figure 19: Daily monitoring of mean wet tropospheric correction difference computed from cycle 001 to cycle 710

Comparison between radiometer and ECMWF wet tropospheric correction highlights the good agreement between the two solutions. This difference is monitored using daily average in order to detect any jump or anomaly (Figure 19), this indicator is stable around 0.00 cm, with a standard deviation value of 0.01 cm.

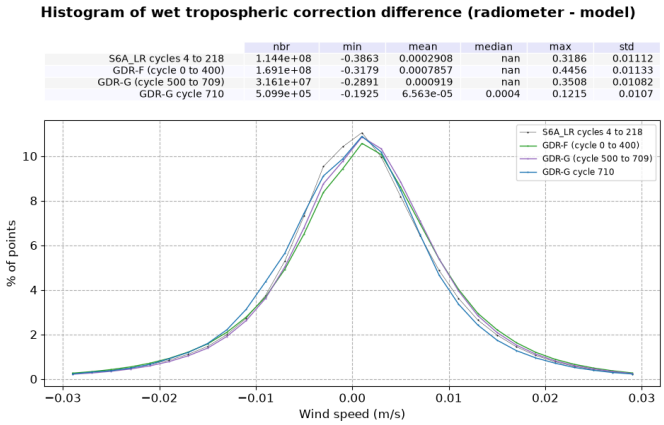


Figure 20: Histogram of wet tropospheric corrections differences

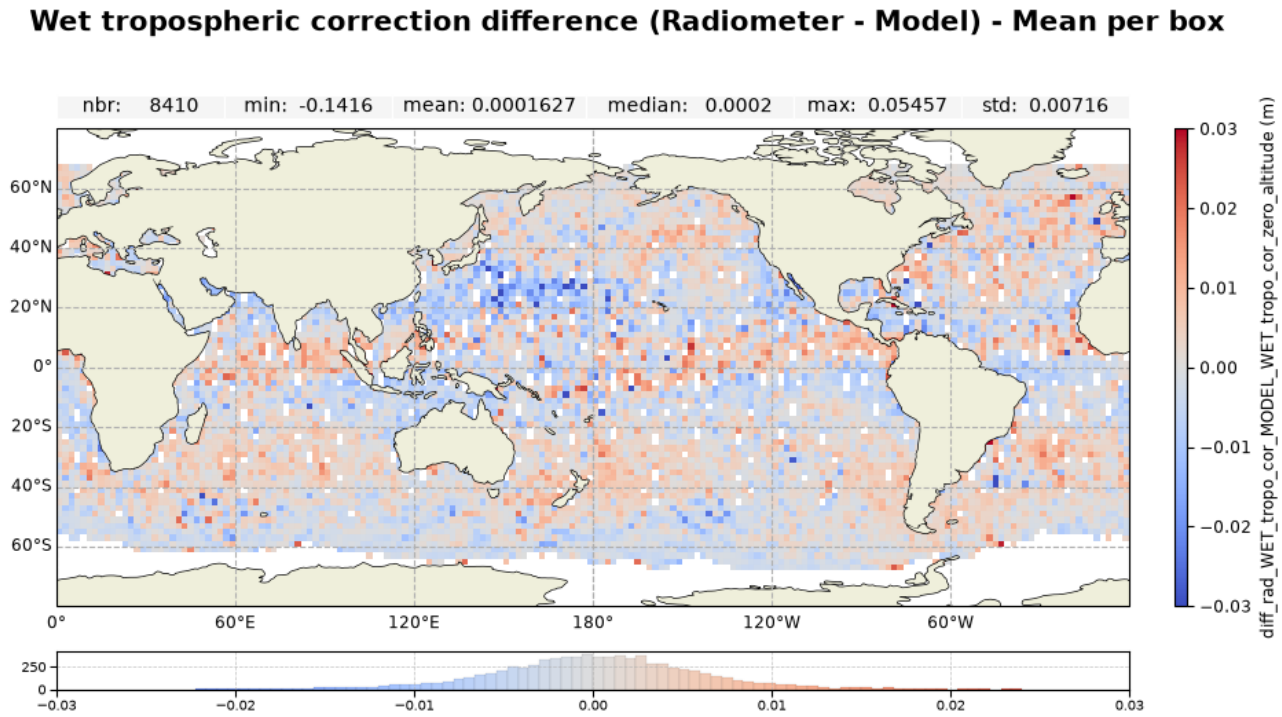


Figure 21: Map of wet tropospheric corrections differences over cycle 710 for Jason-3

5 Crossover Analysis

5.1. Mono mission crossover

Sea Surface Height crossover differences are the SSH differences between ascending and descending passes where they cross each other. Crossover differences are systematically analysed to estimate data quality and the Sea Surface Height (SSH) performances. SSH crossover differences are computed from the valid data, with a maximum time lag of 10 days, in order to limit the effects of ocean variability which are a source of error in the performance estimation. The mean SSH crossover differences should ideally be close to zero and standard deviation should ideally be small.

Nevertheless, SLA varies also within 10 days, especially in high variability areas. Furthermore, due to lower data availability (due to seasonal sea ice coverage), models of several geophysical corrections are less precise in high latitude. Therefore, an additional geographical selection - removing shallow waters, areas of high ocean variability and high latitudes (> |50| deg) - is applied for cyclic monitoring.

After data editing and applying additional geographical selection, the crossover standard deviation over this cycle is about 5.85 cm in MLE4, 6.05 cm in Adaptive.

The maps of the mean differences at crossovers are plotted for the current cycle (top) and from cycle 001 onwards (bottom), for MLE4 (left) and Adaptive (right) on Figure 22.

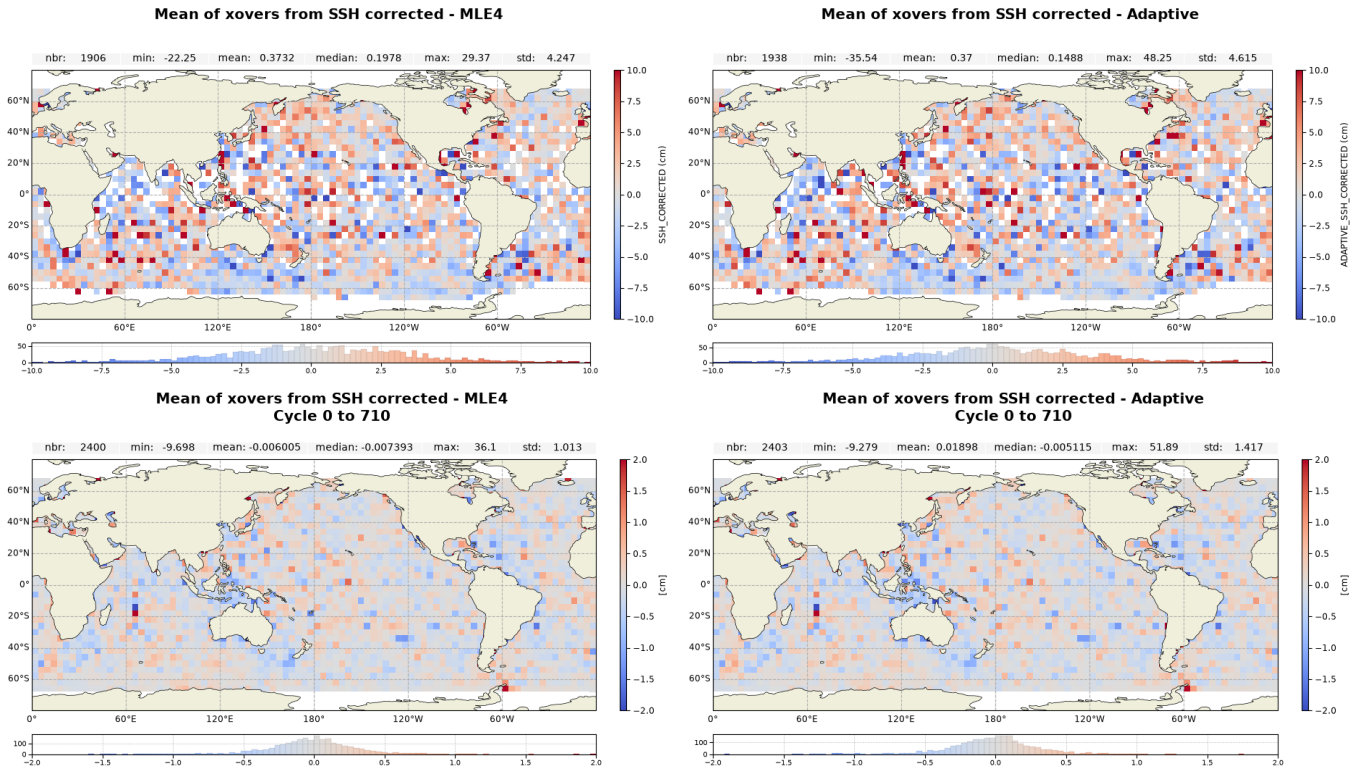


Figure 22: Mean SSH difference at crossovers for Jason-3 MLE4 (left) and Adaptive (right) cycle 710 (top) and from cycle 001 to cycle 710 (bottom)

The mean and standard deviation of SSH differences at crossovers are plotted as a function of time on

a daily basis on Figure 23. The statistics are computed after data editing and using the geographical selection criteria (|latitude| < |50|°, bathymetry < −1000m, ocean variability (computed over several years) < 0.2m). The results are in line between MLE4, and Adaptive data, with the same temporal evolution.

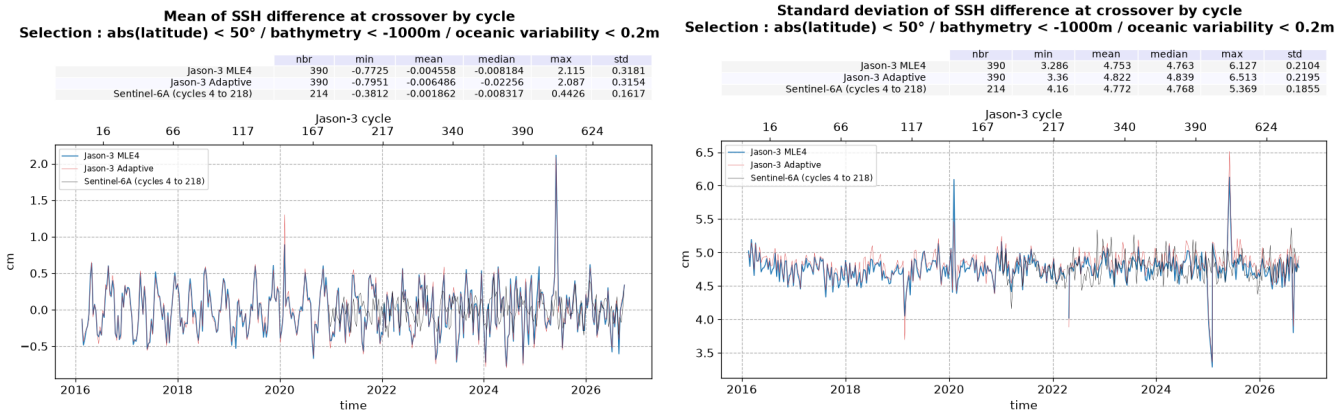


Figure 23: Monitoring of SSH difference at crossovers for Jason-3 MLE4 and Adaptive, and Sentinel-6A LR MLE4 : mean (left) and standard deviation (right), from cycle 001 to 710

6 Sea Surface Height Anomaly

Over this cycle, SSHA is centered around 0.07 cm in MLE4, 0.05 cm in Adaptive (global along-track average).

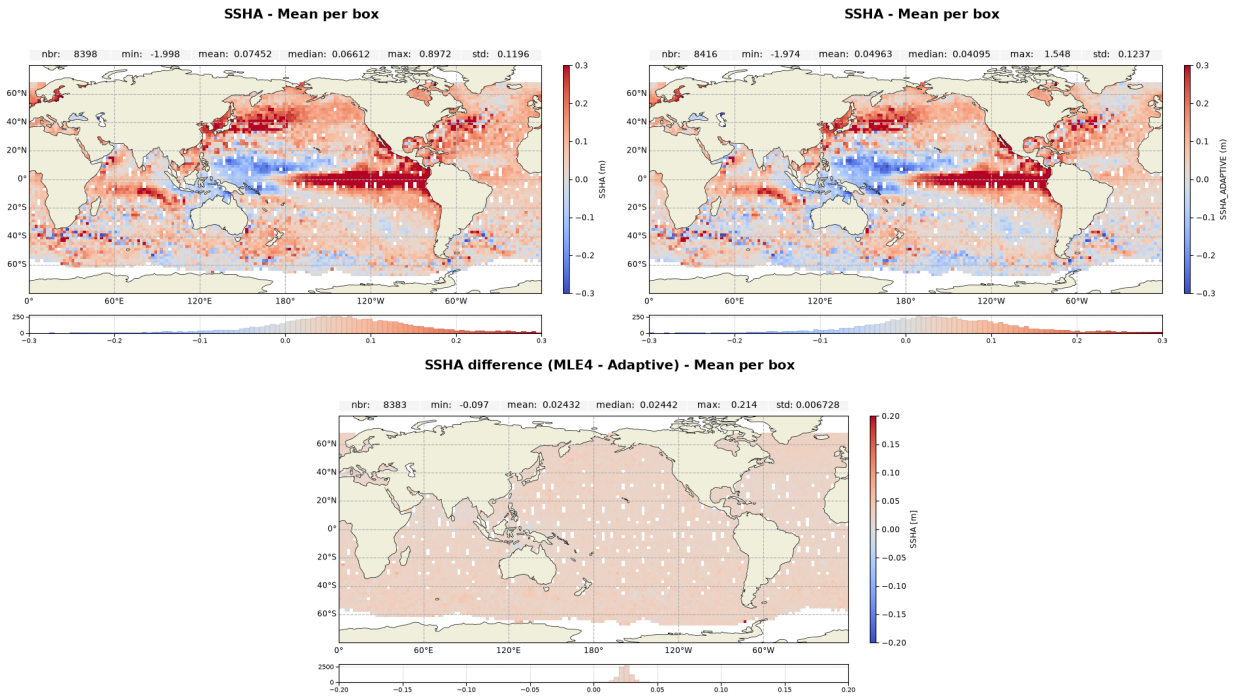


Figure 24: Along-track maps of SSHA over cycle 710 for Jason-3 MLE4 (up left), Adaptive (up right) and difference MLE4-Adaptive (down)

Maps presented on Figure 24 show homogeneous patterns for MLE4 and Adaptive retrackings.

Long term time monitoring helps detecting any jump or drift.
In the plot below, the SSHA daily mean follows the same variations for Jason-3 MLE4 and Adaptive. Along track SSHA standard deviation is stable around 0.11 cm.

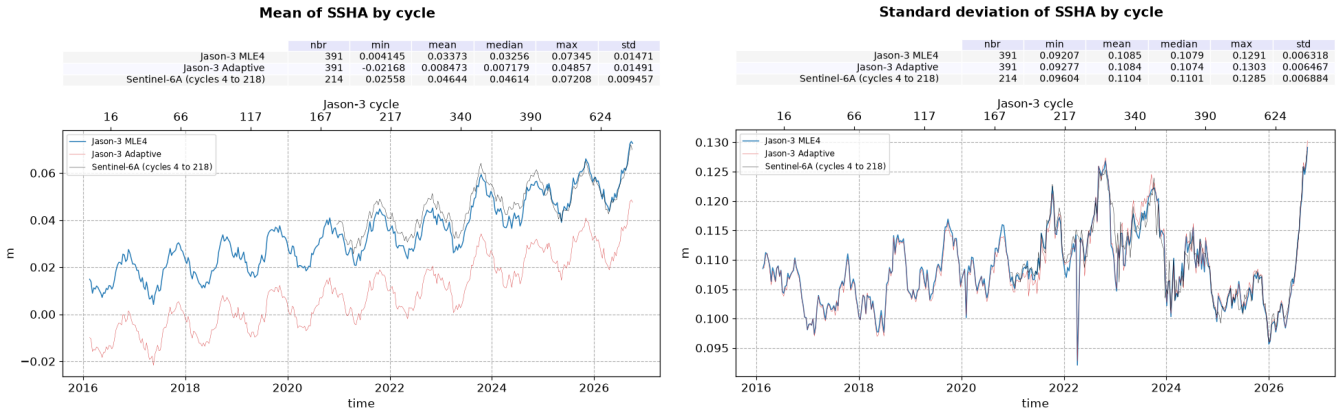


Figure 25: SSHA daily monitoring from cycle 001 to 710, for Jason-3 GDR

7 Mean Sea Level estimations (MSL)

7.1. Global MSL trend

The evolution of the ocean mean sea level can be precisely observed on a continual basis since 1993 thanks to the 5 reference missions: TOPEX/Poseidon, Jason-1 (from may 2002 to october 2008), Jason-2 (from october 2008 to may 2016), Jason-3 (from june 2016 to april 2022) and now Sentinel-6A (since april 2022).

Wet troposphere correction, inverse barometer correction, GIA (-0.3 mm/yr) are applied to calculate the MSL and the data series are linked together accurately thanks to the tandem flying phases. The following global biases are applied:

- -2.260 cm between TOPEX/Poseïdon and Jason-1
- 3.900 cm between Jason-1 and Jason-2
- 2.880 cm between Jason-2 and Jason-3.

An exhaustive overview over possible errors impacting the MSL evolution is given in [5].

Furthermore, annual and semi-annual signals are removed from the time series and a 2-month filter is applied. For more details, see MSL Aviso Website: http://www.aviso.altimetry.fr/msl.

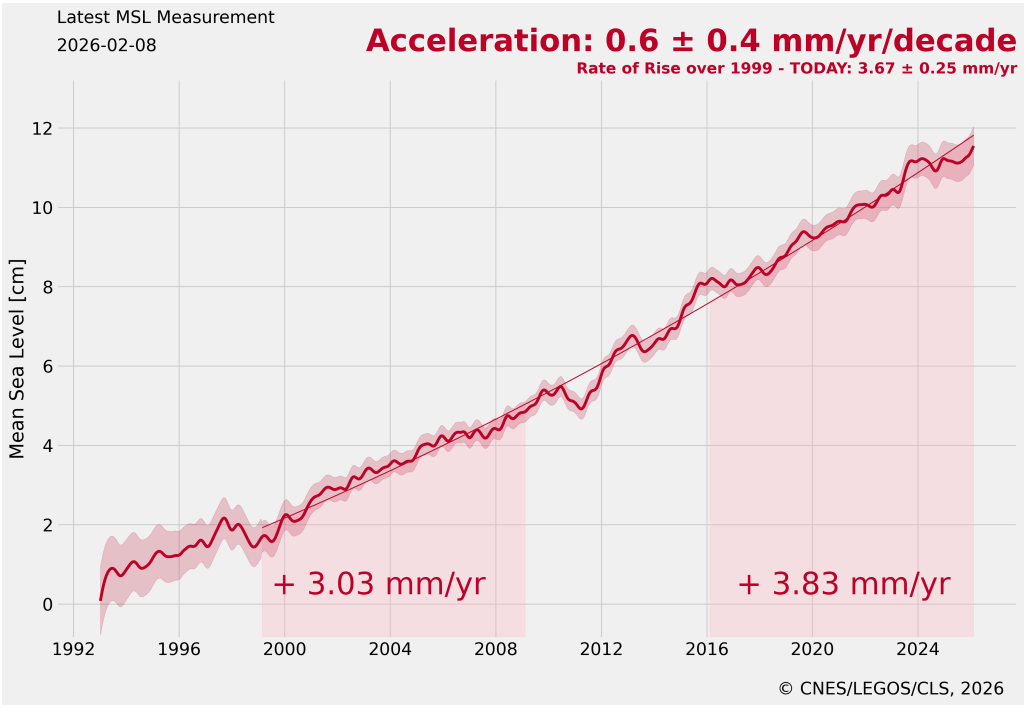


Figure 26: Global MSL trends from 1993 onwards.

7.2. Regional MSL trends

Though mean sea level trend is globally positive, it is inhomogeneously distributed over the ocean. Locally, sea level rise or decline up to $\pm$10 mm/yr are observed on right panel of figure 27. The map of regional MSL trends is estimated from multi-mission grids (Ssalto/DUACS products) in order to improve spatial resolution. Data from Jason-3 mission were introduced in DUACS system end of September 2016 (when Jason-2 moved to its new interleaved orbit).

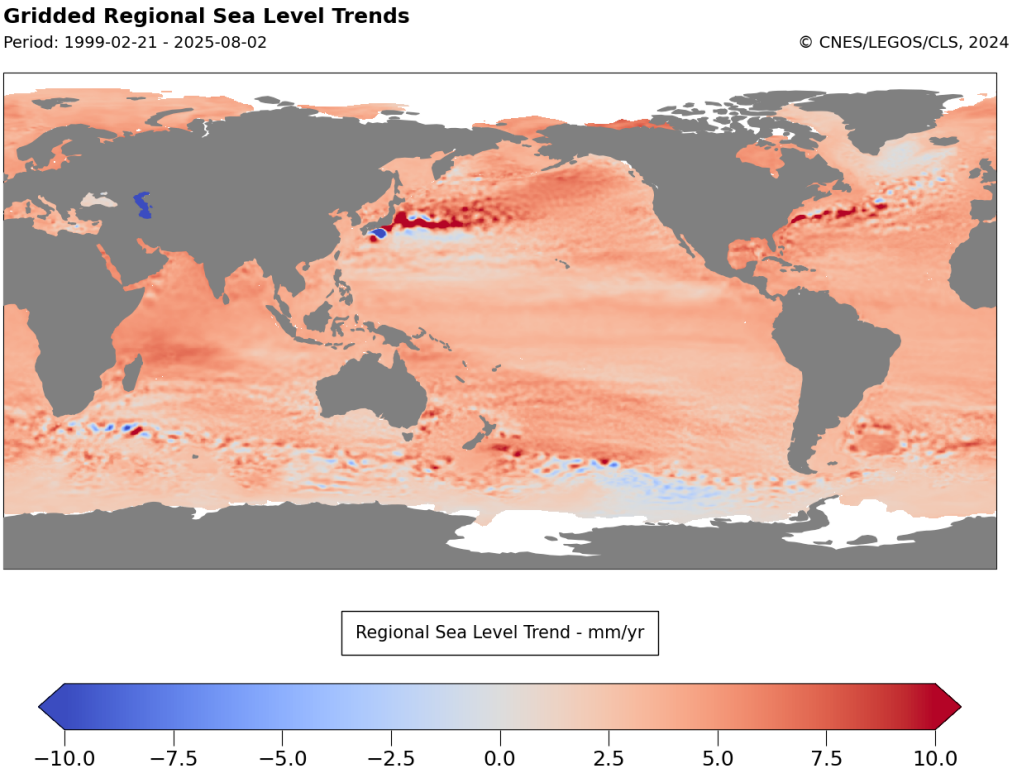


Figure 27: Regional MSL trends from 1999 onwards.

8 Conclusion

These results highlight the good quality of Jason-3 GDR products over ocean. The performances observed at crossovers, the sea level and other parameters derived from both altimeter and radiometer show good metrics and good consistency with the Sentinel-6A reference mission.

References

[1] Description of the mission on AVISO website (https://www.aviso.altimetry.fr/en/missions/current-missions/jason-3.html).

[2] Jason-3 validation and cross calibration activities - Annual Report 2025, Mar 2026 (https://www.aviso.altimetry.fr/fileadmin/documents/calval/validation_report/J3/SALP-RP-MA-EA-23761-CLS-AnnualReport_Jason3_2025.pdf)

[3] Jason-3 validation of GDR-F data over ocean, Dec 2021 (https://www.aviso.altimetry.fr/fileadmin/documents/calval/validation_report/J3/SALP-RP-MA-EA-23480-CLS_Jason3_Reprocessing_Report_v1-2.pdf)

[4] Jason-3 GDR-F user handbook (https://www.aviso.altimetry.fr/fileadmin/documents/data/tools/hdbk_j3.pdf).

[5] M. Ablain, Cazenave, A., Valladeau, G., and Guinehut, S. 2009: A new assessment of the error budget of global mean sea level rate estimated by satellite altimetry over 1993-2008. *Ocean Sci,* **5,** 193-201. Available at http://www.ocean-sci.net/5/193/2009/os-5-193-2009.pdf